(10) Carpenter, R. L.; Kramer, O.; Ferry, J. D. *Macromolecules* **1977**, *10*, 117–9.
(11) Dossin, L. M.; Graessley, W. W. *Macromolecules* **1979**, *12*, 123–30.
(12) Dossin, L. M.; Pearson, D. S.; Graessley, W. W. *Polym. Prepr., Am. Chem. Soc., Div. Polym. Chem.* **1979**, *20*, 224–7.
(13) Kraus, G.; Moczygemba, G. A. *J. Polym. Sci., Part A* **1964**, *2*, 277–88.
(14) Rempp, P.; Herz, J.; Hild, G.; Picot, C. *Pure Appl. Chem.* **1975**, *43*, 77–96 and several references cited therein.
(15) Froehlich, D.; Crawford, D.; Rozek, T.; Prins, W. *Macromolecules* **1972**, *5*, 100–2.
(16) Walsh, D. J.; Allen, G.; Ballard, G. *Polymer* **1974**, *15*, 366–72.
(17) Allen, G.; Holmes, P. A.; Walsh, D. J. *Faraday Discuss. Chem. Soc.* **1974**, *No. 57*, 19–26.
(18) Mark, J. E.; Sullivan, J. L. *J. Chem. Phys.* **1977**, *66*, 1006–11.
(19) Mark, J. E.; Rahalkar, R. R.; Sullivan, J. L. *J. Chem. Phys.* **1979**, *70*, 1794–7.
(20) Llorente, M. A.; Mark, J. E. *J. Chem. Phys.* **1979**, *71*, 682–9.
(21) Ronca, G.; Allegra, G. *J. Chem. Phys.* **1975**, *63*, 4990–7.
(22) Flory, P. J. *J. Chem. Phys.* **1977**, *66*, 5720–9.
(23) Flory, P. J. *Polymer* **1979**, *20*, 1317–20.
(24) Valles, E. M.; Macosko, C. W. In "Chemistry and Properties of Crosslinked Polymers"; Labana, S. S., Ed.; Academic Press: New York, 1977; pp 401–10.
(25) Gottlieb, M.; Macosko, C. W., submitted for publication in *J. Chem. Phys.*
(26) Bueche, A. M. *J. Polym. Sci.* **1956**, *19*, 297–306.
(27) Langley, N. R. *Macromolecules* **1968**, *1*, 348–52.
(28) Pearson, D. S.; Graessley, W. W. *Macromolecules* **1978**, *11*, 528–33.
(29) Berry, J. P.; Scanlan, J.; Watson, W. F. *Trans. Faraday Soc.* **1956**, *52*, 1137–51.
(30) Flory, P. J. *Trans. Faraday Soc.* **1960**, *56*, 722–43.
(31) Carpenter, R. L.; Kramer, O.; Ferry, J. D. *J. Appl. Polym. Sci.* **1978**, *22*, 335–42.
(32) Kramer, O.; Ferry, J. D. *Macromolecules* **1975**, *8*, 87–9.
(33) Joye, D. D.; Poehlein, G. W.; Denson, C. D. *Trans. Soc. Rheol.* **1972**, *16*, 421–45.
(34) Noordermeer, J. W. M.; Ferry, J. D. *J. Polym. Sci., Polym. Phys. Ed.* **1976**, *14*, 509–20.
(35) Hvidt, S. Cand. Scient. Thesis, The University of Copenhagen, 1979.
(36) McLaughlin, W. L.; Miller, A.; Fidan, S.; Pejtersen, K.; Pedersen, W. B. *Radiat. Phys. Chem.* **1977**, *10*, 119–27.
(37) Ferry, J. D. "Viscoelastic Properties of Polymers", 2nd ed.; Wiley: New York, 1970; p 406.
(38) Kramer, O.; Ferry, J. D. *J. Polym. Sci., Polym. Phys. Ed.* **1977**, *15*, 761–3.
(39) Kan, H.-C.; Ferry, J. D. *Macromolecules* **1979**, *12*, 494–8.
(40) Falender, J. R.; Yeh, G. S. Y.; Mark, J. E. *J. Chem. Phys.* **1979**, *70*, 5324–5.
(41) Heilmann, O. J., submitted for publication in *J. Chem. Phys.*
(42) Flory, P. J. *Chem. Rev.* **1944**, *35*, 51–75.

Measurement of the Cluster Size Distributions for High Functionality Antigens Cross-Linked by Antibody

Gustav K. von Schulthess* and George B. Benedek

Department of Physics and Center for Materials Science and Engineering, and the Harvard M.I.T. Division of Health Sciences and Technology, Massachusetts Institute of Technology, Cambridge, Massachusetts 02139

Ralph W. De Blois

General Electric Corporate Research and Development Laboratory, Schenectady, New York.
Received October 16, 1979

ABSTRACT: We have measured, in situ, the evolution of the cluster size distribution of a condensing system of high functionality antigens cross-linked by antibody, using a resistive pulse analizer. The distributions were determined over the full range of values ($0 \leq b < 1$) of the bonding parameter (b) $b = (1 - 1/\bar{n})$ where $\bar{n}$ is the mean number of units in the clusters. The normalized cluster size distributions (X_n/X) are well described by the form $(X_n/X) = (1 - b)e^{-nb}(nb)^{n-1}/n!$. The critical exponents τ, α, and γ_g describing the asymptotic forms of this distribution and its second moment near the condensation point ($b = 1$) can be obtained. We find $\tau = 1.4 \pm 0.15$, $\gamma_g = 2$, and provisionally $\sigma = {}^1/_2$. The experimental distributions are compared with three different classes of theoretical predictions: the solutions of the generalized Smoluchowski kinetic equations, the equilibrium statistical distributions, and the theories of three-dimensional percolation.

The cluster size distribution of interacting particles plays a central role in the characterization of condensing systems. Such cluster size distributions occur in the study of: organic polymer reactions,[1-4] antibody–antigen agglutination reactions,[5-7] percolation processes,[8-10] gas–liquid and magnetic order–disorder phase transitions,[11-13] and colloidal[14] and aerosol[15] suspensions. The theories of the cluster size distribution usually assume thermodynamic equilibrium among the clusters for each value for the extent of the reaction.[2] Recently, modern theories of critical phenomena have drawn attention to the use of static scaling laws and critical exponents to describe the divergence of the moments of the equilibrium cluster size distributions near the critical condensation point.[16-18] On the other hand, following von Smoluchowski,[19] a number of authors[15,20-22] have focused on the kinetics of such reactions and have computed the temporal evolution of the cluster size distributions, using various mathematical forms for the interparticle reaction rates.

We report measurements of the distribution of cluster sizes, using as the interacting particles polystyrene latex spheres (diameter 0.235 μm) upon whose surface the antigen human serum albumin (hSA) has been covalently bonded. These antigen coated carrier particles (units) are cross-linked by complementary bivalent antibody molecules—goat anti-hSA introduced into the solution. The cluster size distribution was measured by using the Nanopar resistive pulse particle size analyzer devised and developed by De Blois and Bean.[23,24] This analyzer permits the measurement of the number of units in the individual clusters within our reaction mixture without disturbing the reaction kinetics.

Our reacting particles and the measurement method taken together provide a unique system for the quantitative investigation of the cluster size distribution. The use of antigen-coated carrier particles rather than polyfunctional organic molecules (units) has the effect of increasing the size of the units from ~100 Å to ~2000 Å and in-

0024-9297/80/2213-0939$01.00/0 © 1980 American Chemical Society

creasing their functionality from f ~ 4 to ~10^3. The increase in size permits the detection and sizing of the individual clusters by the resistive pulse analyzer, while the great increase in functionality permits a convenient mathematical simplification of the theoretical form of the cluster size distributions. The characteristic time for the kinetic approach to steady state conditions for this reacting system is ~5 h while the time required for the measurement of the distribution is ~3 min. Thus the distribution changes a negligible amount during the measurement time. This, combined with the fact that the resistive pulse analyzer does not disrupt the reaction process, permits a continuous, in situ, measurement of the temporal evolution of the cluster size distributions during the progress of the reaction.

The agglutination of dense solutions of coated carrier particles at a high concentration of cross-linking (agglutinator) molecules is widely used as a scheme for clinical immunoassay. There the appearance of a visible precipitate is used to detect the cross-linking agglutinator molecule (e.g., antibody). In a series of papers[25-28] we have used quasielastic light scattering spectroscopy and classical light scattering anisotropy measurements to detect small changes in the cluster size distributions, using low concentrations of carrier particles and hence very low levels of agglutinator. The observed changes in cluster size distributions provide a very sensitive immunoassay. In fact, the present detection method also may be used as an immunoassay method[29] which is as sensitive as our best optical methods and is comparable to the sensitivity of the ratio-immunoassay methods.

Experimental Section

Materials and Methods. (a) Materials. Carboxylated Dow Chemical Co. latex spheres of diameter 0.235 μm upon whose surface the antigen, human serum albumin (hSA), had been covalently bound by a carbodiimide reaction were kindly provided through the courtesy of Dr. Hans Hager of the Hoffmann-La Roche Co., Nutley, N.J. The stock solutions, as provided, contained about 75% monomers and 25% aggregates by weight. We removed the aggregates and obtained solutions containing at least 97% monomer by weight by the following centrifugal separation method. Aliquots (50 μL) of the latex sphere stock solution were layered on top of ~0.8 mL of a 10% sucrose solution (by weight) in 1 mL test tubes. The density of the polystyrene latex is 1.05 g/cm^3 while that of the 10% sucrose solution is 1.04 g/cm^3. This small difference produces a low sedimentation velocity in the centrifuge. The test tubes were spun at 200 g for 15–20 min. After this time a layer containing latex sphere monomers had migrated about 3–5 mm into the sucrose solution, while the aggregates were found in a clearly separate distribution deeper in the solution. The clearly distinct monomer layer was then withdrawn with a syringe and used for subsequent measurements. The concentration of hSA coated spheres used in our experiments was ~10 μg/mL (1.5 × 10^9/mL). This was determined by dry weighing and by use of the resistive pulse technique.[23,24]

Solutions containing goat anti-hSA antibodies with a concentration of 9.6 mg/mL as determined by precipitin analysis were kindly provided by Dr. Hans Hager of the Hoffmann-La Roche Co. and used as the cross-linking agent in our studies.

The agglutination reactions were performed at room temperatures (24 ± 2 °C) after diluting the latex spheres and the antiserum to the desired concentrations with 0.1 M Tris buffer at pH 8.15. Buffer and diluted antibody were both filtered through 0.2 μm Nuclepore filters obtained from the Nuclepore Corp., Pleasanton, Calif. The hSA coated spheres were incubated with the antibody promptly after suitable dilution of the latter, thus initiating the agglutination reaction. The Debye shielding length in our solutions is determined from the ionic strength of the Tris buffer to be ~5 Å.

The specificity of the antibody for producing the agglutination reaction was checked by incubating the hSA coated spheres with rabbit antihuman chorionic gonadotropin (hCG) antibody. In this case, no aggregation was observed for concentration ranges of latex spheres and antibody of interest over a period of up to 3 days—the period of observation for the agglutinating samples. A similar negative result was found if latex spheres coated with hCG antigen were incubated with goat anti-hSA antibody.

(b) Experimental Method. The distribution of cluster sizes was measured by using a Nanopar resistive pulse particle size analyzer.[23,24] In our instrument the reaction mixture was separated into two regions by a polycarbonate film (thickness 8.0 μm) which is pierced by a single cylindrical pore (diameter ~2 μm). Pores are produced by etching damage tracks made by fission fragments from ^{252}Cf. The pore permits the flow of solvent and solute (ions and clusters) between the two parts of the chamber. A flow of electrical current carried by the mobile ions through the pore is established by ~1.8 V potential difference impressed across the pore by a pair of electrodes. A simple circuit maintains an essentially constant electric current across the pore. A small hydrostatic pressure difference (~4 in. of water) across the pore results in a flow of the clusters of cross-linked polystyrene spheres across the pore. The density of particles is low enough that on the average the number of particles contained in a volume of the pore is at most 0.07. Thus it is quite unlikely that the pore contains more than one cluster at a time. On the average a cluster remains in the pore for ~0.5 ms. An insulating particle cluster in the pore distorts the ion current in such a way as to increase the electrical resistance of the pore. The change in pore resistance is directly proportional to the volume of solvent displaced by the cluster and hence to the number of units in the cluster for linear dimensions of the cluster less than about four-tenths of the pore diameter.[23,24] Under these conditions, the amplitude of the voltage change ΔE produced by the passage of a cluster through the pore is proportional to the number of particles in the cluster. The distribution of pulse heights produced by the random passage of different size clusters can then be accumulated electronically and converted into a distribution which displays the number of clusters counted as a function of the measured voltage change ΔE. This distribution is quasicontinuous in the sense that each peak associated with an aggregate of order n has a finite width. Contributions to this width come from: intrinsic polydispersity in the latex sphere's radius, entrance and exit effects,[23,24] and second-order effects on ΔE associated with the orientation of asymmetrical clusters.[30] In the following data analysis section we shall describe the procedure used to deconvolve this continuous distribution of overlapping peaks so as to obtain a discrete histogram of the number of clusters vs. the order number n.

(c) Data Analysis. The experimentally observed distribution of pulse heights contains clearly defined peaks for values of n usually from n = 1–6. For larger values of n, the distribution is monotonically decreasing. The value of ΔE at the maximum of each resolvable peak is found to be an integral multiple of the value ΔE_1 corresponding to the monomer peak, thus confirming the linear relationship between ΔE and the order of the cluster at least for $1 \leq n \leq 6$. In view of this, we assume this linear relationship continues for higher n and divide the ΔE axis into bins whose centers are at $p\Delta E_1$, where p = 1, 2, 3..., and whose boundaries are at $p\Delta E_1 \pm \Delta E_1/2$. All the counts falling within each bin are taken to be associated with a cluster having a value of $n = p$. This simple deconvolution procedure provides a histogram for the cluster size distribution which is in very good agreement with that obtained by using a more sophisticated deconvolution involving overlapping Gaussians with adjustable peak heights and widths.[31] Using this procedure, we obtained histograms of the number of clusters (N_n) vs. the order (n) for a finite counting interval (usually 200 s).

Let N_0 be the total number of monomers which would move through the pore in a given time in the absence of aggregation. N_0 can be determined experimentally in two different ways. In the first way we allow an unaggregated sample of the carrier particles to pass through the pore under the influence of a pressure gradient equal to that applied to the aggregating sample. Call the value so obtained $(N_0)_1$. In the second method we can actually count the number of units in all the clusters, using the conservation of mass condition. This gives $(N_0)_2$ as

$$(N_0)_2 = \sum nN_n \qquad (1)$$

provided that all the material is in the solution phase. In this

second method possible variations in the flow rates are unimportant.

The theoretical measure of the cluster size distribution is the ratio X_n/X where X_n is the mole fraction of clusters of order n in the solution and X is the total mole fraction of latex spheres initially put into the solution. From the definition of N_n and N_0 we have

$$X_n/X = N_n/N_0 \tag{2}$$

N_n is found directly from the data analysis of the experimental histograms, and N_0 can be obtained in either of the two ways mentioned above. In fact, for those distributions in which $\bar{n} \equiv (\sum nX_n/\sum X_n) \leq 4$, we were able to show experimentally that $(N_0)_1 = (N_0)_2$ to within 10%. On the other hand, for $\bar{n} > 4$ the distribution for N_n falls off so slowly that an accurate value of $(N_0)_2$ is not possible. In calculating X_n/X we used $N_0 = (N_0)_1$ for all the distributions for which $\bar{n} > 1.5$ and $N_0 = (N_0)_2$ for all the distributions for which $\bar{n} \leq 1.5$ so as to obtain the most accurate estimates of X_n/X.

Each of the X_n distributions can be characterized by an experimentally measured parameter b defined as

$$b = \left(1 - \frac{\sum_n X_n}{X}\right) \tag{3a}$$

or

$$b = \left(1 - \frac{\sum N_n}{N_0}\right) \tag{3b}$$

In the case where the clusters are branched trees having no cyclic structures, and if only the solution phase is present, then b has a simple physical interpretation. It is simply the mean number of bonds per latex particle. This is seen as follows. Since $(n-1)$ is the number of bonds in a branched cluster, the number of bonds per particle in all the clusters is $\sum(n-1)X_n/X$. If all the material is in solution phase clusters, then $\sum nX_n = X$, and hence the mean number of bonds per particle is equal to the quantity b defined in eq 3.

Under the conditions above, one can also relate b to $\bar{n}$, the mean cluster order number (or the mean cluster "size"). $\bar{n}$ is defined as

$$\bar{n} \equiv \sum nX_n/\sum X_n$$

If all the particles are in the clusters in solution, then $\bar{n} = X/\sum X_n = 1/(1-b)$. Hence we see that

$$b = (1 - 1/\bar{n}) \tag{4}$$

At the beginning of the aggregation process $b = 0$. In the extreme case of a heavily aggregated sample $\bar{n} \to \infty$ and $b \to 1$. Thus the entire range of b is $0 \leq b < 1$.

Results

We determined the N_n histograms as a function of time (t) for a wide range of the following: mole fraction of latex spheres (X), concentrations of antibody $[ab]_0$, and solution ionic strengths (I). These system variables were changed within the following domains: $10^{-13} < X < 10^{-14}$, 10^{-7} M/L $> [ab]_0 > 10^{-11}$ M/L, 0.1 M/L $> I >$ 0.025 M/L. The range of times studied was 3 min $< t <$ 48 h. From the experimentally measured N_n and N_0 we computed the value of the parameter b, using eq 3b for each observed distribution. This distribution parameter b is of course functionally related to each of the system variables, viz., $b = b(X,[ab]_0,I,t)$. We were able to obtain closely similar values of b, using widely different combinations of the system variables X, $[ab]_0$, I, and t. After extensive and careful analysis[31] of the data, we found that the detailed form of the cluster size distributions (N_n/N_0) was determined solely by the value of b itself and was independent of the particular combination of the system variables $(X,[ab]_0,I,t)$ which produced that value of b. In view of this finding we shall present our findings on the cluster size distributions X_n/X as functions only of b and n. The detailed dependence of b upon X, $[ab]_0$, I, and t individually will be described in another paper.

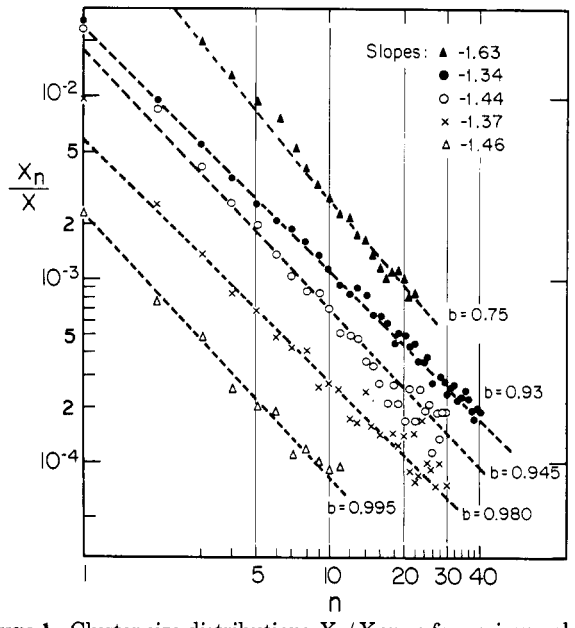

Figure 1. Cluster size distributions X_n/X vs. n for various values of the parameter $b = (1 - \sum X_n/X)$ equal to or greater than 0.75.

In Figure 1 the experimental points showing X_n/X are plotted vs. n for values of b in the range $0.75 \leq b \leq 0.995$. The linearity of X_n/X vs. n on these log–log coordinates shows that, in the observed range of n values, $X_n/X \propto n^{-\tau}$. This power law is an empirical representation of our data, yet it is consistent with theoretical expectations which are discussed below. The values of the exponent τ for each distribution were determined from a straight-line fit (dotted lines) and displayed in the figure inset on the upper right. It will be noted that as $b \to 1$, $\tau \simeq 1.4 \pm 0.15$. Further data must be taken to establish whether or not τ is in fact systematically less than 3/2 as suggested by the slopes shown in the inset.

For values of $b < 0.75$ the values of n for which X_n/X are measured most accurately are typically less than $n = 5$. Thus, we find it more convenient to present the cluster size distributions as functions of b for fixed values of n, $1 \leq n \leq 4$. In Figure 2 we plot as experimental points our measurements of nX_n/X vs. b for $n = 1$–4. The error estimates are indicated by bars on selected experimental points.

The cluster size distributions found above can be represented well by the following formula, whose theoretical origins will be discussed in the next section.

$$\frac{X_n}{X} = \frac{(1-b)e^{-nb}(nb)^{n-1}}{n!} \tag{5}$$

A useful asymptotic form for this distribution valid as $b \to 1$ is:

$$\left(\frac{X_n}{X}\right) \underset{\substack{n \gg 1 \\ b \to 1}}{=} \frac{1}{(2\pi)^{1/2}} \frac{(1-b)}{b} \frac{1}{n^{3/2}} F(n,b) \tag{6}$$

where

$$F(n,b) = (be^{1-b})^n \tag{7a}$$

Asymptotically, as $b \to 1$ we can write $b = 1 - \epsilon$, and

$$F(n,b) \underset{b \to 1}{\simeq} \left(1 - \frac{\epsilon^2}{2} + \ldots\right)^n \simeq \left(1 - \frac{n\epsilon^2}{2}\right) \tag{7b}$$

Thus $F(n,b) = 1$ as $b \to 1$ provided that $n \ll 2/(1-b)^2$.

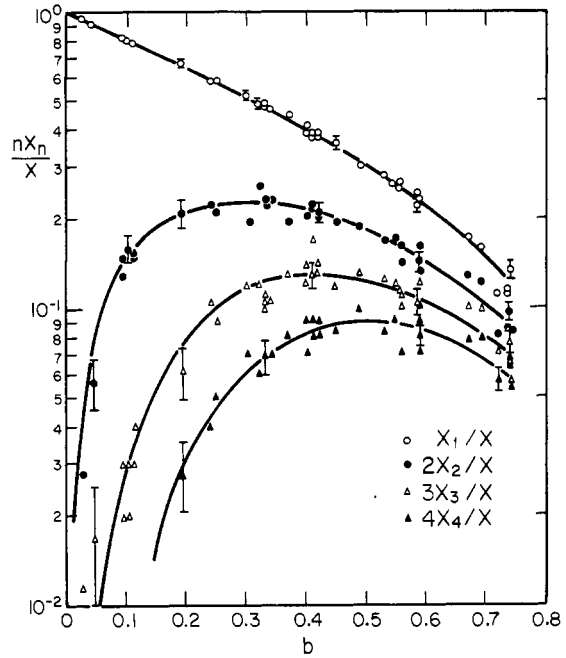

Figure 2. Cluster number distributions nX_n/X vs. b for n = 1–4. The solid lines are obtained by using eq 5.

These conditions on n and b are in fact satisfied for our data for $0.9 \leq b \leq 1.0$ and $n < 40$. Thus we see that eq 5 predicts $X_n/X \rightarrow n^{-3/2}$, over the region of n of our data, as $b \rightarrow 1$. This is borne out by the experimental data shown in Figure 1.

In Figure 3 we show as solid lines the predicted values of X_n/X obtained by using eq 6 with $F = 1$ for $b \geq 0.93$. For each calculated distribution the value of b used was that obtained from the data, using eq 3a. In the case of $b = 0.75$, the exact formula eq 5 was used.

In Figure 2 we plot as solid lines nX_n/X vs. b for n = 1–4 for values of $0 < b \leq 0.75$ and show the close matching of the experimental data with these lines. A particularly stringent quantitative test of the accuracy of eq 5 in describing the data can be made as follows. We can rewrite eq 5 as follows

$$\left(\frac{n!}{n^{n-1}}\left(\frac{b}{1-b}\right)\frac{X_n}{X}\right)^{1/n} = be^{-b} \tag{8}$$

Thus, expressing our experimental data on X_n/X in the form shown on the left-hand side of eq 8 and plotting it as a function of b should provide the same function, be^{-b}, for each value of n. We carried out this procedure for n = 1–4 and the results are shown as points in Figure 4. The solid lines shown are the function be^{-b}. Clearly the data in Figure 4 agree quite satisfactorily with the form of eq 8 for X_n/X over the entire range of $0 < b < 1$. The comparisons between eq 5 and the data shown in Figures 2 and 3 as well show this equation to provide a quite satisfactory representation of the measured cluster size distributions.

Discussion

Recent theoretical investigations[16,17] of the cluster size distributions emphasize the characterization of the distributions and their moments in the vicinity of the condensation or gelation point (b_c) in terms of certain exponents τ, σ, α_g, β_g, γ_g which occur in the precolation theory. For values of $b > b_c$, both solution and gel phases can coexist. For $b < b_c$ only the solution phase is present. These theories use as a measure of the distance from the condensation point the parameter ϵ where

$$\epsilon = (b_c - b)/b_c \tag{9}$$

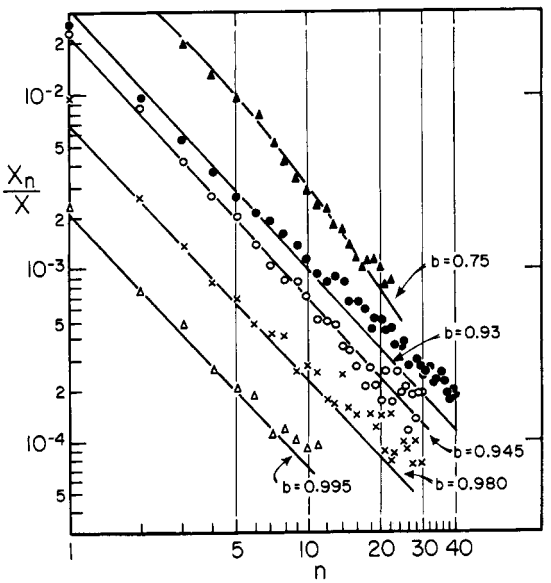

Figure 3. Comparison between the prediction of eq 6 and 5 and the experimental values of X_n/X. Equation 5 is used for the b = 0.75 distribution and the asymptotic form, eq 6, is used for $b \geq 0.93$.

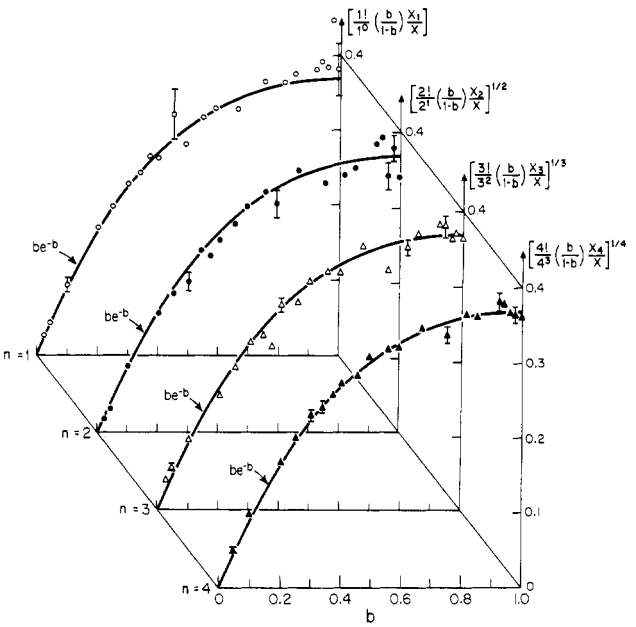

Figure 4. A comparison between the experimental data on X_n/X vs. b and the theoretical form given in eq 8 for values of n = 1–4.

Using this definition of ϵ, we have defined the exponents τ and σ in terms of the cluster size distribution X_n/X as follows[16]

$$X_n/X \underset{b \rightarrow b_c}{\equiv} q_0 n^{-\tau} F(\epsilon n^{\sigma}) \tag{10}$$

where q_0 is a constant, and F is an analytic and positive function of its argument $Z \equiv \epsilon n^{\sigma}$. The exponents α_g, β_g, and γ_g which describe the solution–gel transition are defined in terms of the various moments of the cluster size distribution as follows. The zeroth moment of the distribution ($\mathcal{N}$) is

$$\mathcal{N} \equiv \sum_{n=1}^{\infty} X_n/X \tag{11a}$$

Physically $\mathcal{N}$ is the total number of clusters regardless of size divided by the total number of units X. The exponent α_g is determined by the asymptotic behavior of $\mathcal{N}$ as the

Table I
Exponents Characterizing the Cluster Size Distributions

	exponents					
	b_c	τ	σ	α_g	β_g	γ_g
present experiments	1	1.4 ± 0.15	0.5			2
kinetic distribution for $a_{nn'} = B(n + n')$; statistical distribution for $\mathcal{A}R\mathcal{B}_{f-1}$ monomers	1	1.5	0.5			2
kinetic distribution for $a_{nn'} = Cn \cdot n'$; statistical distribution for $R\mathcal{A}_f$ monomers $f \to \infty$	1/2	2.5	0.5		1	1
percolation theory $d = 3$		2.18	0.46	−0.6	0.39	1.8

gel point is approached, i.e., as $\epsilon \to 0$, according to the equation

$$(\mathcal{N} - \mathcal{N}_0) \propto |\epsilon|^{2-\alpha_g} \tag{11b}$$

Here $\mathcal{N}_0$ is a function which is analytic in near $\epsilon = 0$. α_g is the exponent which describes the power law dependence of the nonanalytic part of $\mathcal{N}$, if any such part exists.

The first moment (S) of the cluster size distribution is the fractional number of units in the solution phase:

$$S = \sum_{n=1}^{\infty} nX_n/X \tag{12a}$$

For $b < b_c$ all the material is in the solution phase and $S = 1$. For values of b exceeding the critical condensation point, the normalization of S fails and the missing material appears in the gel phase. The gel fraction G is defined as

$$G = (1 - S) \tag{12b}$$

and the exponent β_g is defined[16] in terms of the dependence of G upon ϵ near $\epsilon = 0$, viz.,

$$G \propto |\epsilon|^{\beta_g} \tag{12c}$$

The second moment of the distribution, or the degree of polymerization, DP_w, is defined[16] as

$$DP_w = \sum_{n=1}^{\infty} n^2X_n/X \tag{13a}$$

The exponent γ_g is defined in terms of the dependence of DP_w on ϵ as $\epsilon \to 0$, viz.,[16]

$$DP_w \propto |\epsilon|^{-\gamma_g} \tag{13b}$$

It is important to recognize that the exponents α_g, β_g, and γ_g as defined above following Stauffer[16] are theoretically and numerically different from the exponents α, β, and γ which describe the divergence of the specific heat, the shape of the coexistence curve, and the divergence of the compressibility in the vicinity of the critical point for the gas–liquid phase transition. There are two reasons for this difference. The first is that in the case of the gas–liquid phase transition the fractional distance from the critical point is $|(T_c - T)/T_c|$ and the analogous variable for this in the solution–gel transition is not ϵ but rather $\zeta \equiv |(X_1 - X_{1_c})/X_{1_c}|$ where X_1 is the mole fraction of monomers and X_{1_c} is the maximum value of X_1 which obtains when $b \to b_c$. The second difference is that the free energy in the percolation or gelation problem has a different symmetry property upon reversal in sign of the order parameter than does the free energy of the gas–liquid phase transition.

In Table I we list in row 1 the value of b_c and the values of the exponents which can be deduced from our experiments. The distribution we have found to describe our data, i.e., eq 5, has as its condensation point the value $b_c = 1$. Thus for this distribution $\epsilon = (1 - b)$. In our distribution the critical condensation point $b_c = 1$ occurs at the limit of the possible values of b. As a result one can asymptotically approach the condensed phase but cannot enter into it. This corresponds to a phase transition at $T = 0$. As a result no gel phase occurs and the exponent β_g cannot be obtained from our data. In column 2 we present the value of τ obtained from our data in Figure 1.

We can obtain σ from the form of X_n/X as $b \to 1$. Using eq 10, 6, and 7, we see that $\epsilon^2 n^{2\sigma} \to \epsilon^2 n$. This implies $\sigma = 1/2$. We place this value of σ in column 3 of Table I with the reservation that eq 7 for F only applies for $\epsilon \geq 0$ and so the ϵ^2 dependence expressed in eq 7b cannot be examined experimentally for both negative and positive values of ϵ.

Using eq 11a for $\mathcal{N}$ and eq 5 for X_n/X, we can compute $\mathcal{N}$ vs. $\epsilon = (1 - b)$. This gives

$$\mathcal{N} = (1 - b) = \epsilon \tag{14}$$

Thus $\mathcal{N}$ is analytic in ϵ and the exponent α_g cannot be deduced from the distribution of eq 5. Accordingly, a gap is left in column 4.

Using eq 13a and eq 5, we can compute DP_w. This gives

$$DP_w = 1/(1 - b)^2 = 1/\epsilon^2 \tag{15}$$

Thus $\gamma_g = 2$, and this is included in column 6, row 1, of Table I.

We now examine theoretical predictions for the form of the cluster size distributions keeping in mind that our system evolves in time and that therefore a kinetic description should be considered. In fact under the conditions of our experiment[31] the reaction between units appears to be unidirectional: once particles are bound they do not dissociate. To describe the kinetics of the reaction we regard the development of the clusters as the result of "bimolecular" encounters. We may define a bimolecular reaction rate constant $a_{n'n}$ in terms of the rate of formation of an $n + n'$ mer in the presence only of n mers and n' mers. Thus if X_n is the mole fraction of n mers present, a bimolecular reaction implies that:

$$\dot{X}_{n'+n} = a_{n'n}X_{n'}N_n \tag{16}$$

where $a_{n'n} = a_{n'n}$. The magnitude of $a_{n'n}$ and its dependence on n,n' is controlled by the detailed form of interaction between units and by the physicochemical parameters of the solution.

The unidirectional kinetic equations for the distribution function X_n have the form:[15,19]

$$\dot{X}_n = \tfrac{1}{2}\sum_{n'=1}^{(n-1)} a_{(n-n')n'}X_{n-n'}X_{n'} - \sum_{n'=1}^{\infty} a_{nn'}X_nX_{n'} \tag{17}$$

In this generalized von Smoluchowski equation,[15] the first terms on the right-hand side represent the rate of formation of n mers from all possible pairs of clusters which together contain n units. The second term on the right-hand side of eq 17 represents the rate of loss of n mers due to their combination with all other possible n' mers. Analytic solutions for eq 17 exist if the $a_{n,n'}$'s have the following general form

$$a_{n'n} = A + B(n + n') + C(n \cdot n') \tag{18}$$

and these solutions have been reviewed by Drake.[15] These solutions have the property that at each instant of time and for fixed A, B, and C, X_n/X is a function only of n

and b where $b = \sum(n-1)X_n/X$ and is identical with that defined above in eq 3. b obeys a differential equation in time whose functional form is determined by the relative magnitudes of A, B, and C. Thus the structures of the solutions of these kinetic equations have the interesting property found experimentally, namely, that at each point in time the distribution can be characterized with the single parameter b.

In the particular case where $a_{nn'} = B(n + n')$, i.e., $A = C = 0$, Golovin[15,21] has shown that the cluster size distributions X_n/X obtained from the kinetic equations have precisely the same form as that given in eq 5 which fits our data quite well. Thus our experimental distributions are consistent with those obtained theoretically from unidirectional kinetics provided that the bimolecular reaction rate constant has the simple form $a_{n,n'} = B(n + n')$.

The experimentally observed distribution (eq 5) can also be obtained theoretically, assuming chemical equilibrium is achieved between each of the n mers in the distribution. Indeed, Flory (ref 2, p 365) has obtained the form of the cluster size distribution for condensing monomers of the type $\mathcal{A}R\mathcal{B}_{f-1}$. Each such monomer has exactly one $\mathcal{A}$ site and $(f-1)$ $\mathcal{B}$ sites, and linkage occurs only between $\mathcal{A}$ and $\mathcal{B}$ sites. It can be shown[31] that in the limit $f \gg n$ the theoretical cluster size distribution for such monomers has precisely the form of our experimental distribution, eq 5. The critical exponents corresponding to this distribution are listed in row 2 of Table I.

It might be argued that the attachment of an antibody to an antigen on the surface of the carrier particle produces a monomer of the $\mathcal{A}R\mathcal{B}_{f-1}$ form. However, analysis[26] of the number of bound antibodies shows that over the range of our experiments the number of antibodies and hence $\mathcal{A}$ type sites ranges from a minimum of 10 to a maximum of $\sim f$. To obtain the form of eq 5 in the limit $f \gg n$, it is in fact essential that there be exactly a single $\mathcal{A}$ site on the carrier particle.

The theoretical distribution which is most widely used in the description of the solution–gel transition is the Flory–Stockmayer distribution[2,3] describing the condensation of monomers of the form $R\mathcal{A}_f$. Each such monomer has f $\mathcal{A}$ sites which are each available for cross-linking between monomers. It can be shown[32] that in the limit $f \gg n$ the Flory–Stockmayer distribution has the form

$$\frac{X_n}{X} = \frac{e^{-2bn}(2nb)^{n-1}}{nn!} \tag{19}$$

This distribution has markedly different properties from that corresponding to the $\mathcal{A}R\mathcal{B}_{f-1}$ monomers (with $f \gg n$), particularly as regards the solution-gel transition. We summarize these properties in row 3 of Table I. The Flory–Stockmayer distribution has a critical condensation point at $b = 1/2$. The various moments of the distribution can be calculated[33] and one obtains:

$$N = \tfrac{1}{2} + (\tfrac{1}{2} - b) \tag{20a}$$

$$G \underset{b \to 1/2}{=} 4(b - \tfrac{1}{2}) \tag{20b}$$

$$\mathrm{DP_w} = \tfrac{1}{2}/(\tfrac{1}{2} - b) \tag{20c}$$

The corresponding critical exponents are listed in Table I. Comparison of these theoretical results for the $R\mathcal{A}_f$ system with those of the $\mathcal{A}R\mathcal{B}_{f-1}$ system with $f \to \infty$ shows that the critical exponents near the condensation point depend markedly on the structural restrictions on the combinatorial possibilities allowed between monomers.

The distribution of eq 19 also results from a kinetic analysis. If $A = B = 0$ in eq 18, i.e., if the reaction rate constant $a_{nn'}$ has the form $a_{nn'} = Cn{\cdot}n'$, then the solution[3,15,20] of the kinetic eq 17 has the Flory–Stockmayer ($f \to \infty$) form given in eq 19.

Finally, in the fourth row of Table I we list theoretically calculated values of the critical exponents from three-dimensional percolation theory.[16] The predicted value of τ is clearly outside the limit of error found in our experimental determination of τ.

Conclusions

The present experiments provide a remarkably detailed measurement of the cluster size distributions of a model system of highly polyfunctional units undergoing condensation. The distributions X_n/X are characterized by a single parameter b, the mean number of bonds per unit, and the distributions have been measured over the full range of values of b, $0 \le b < 1$. The critical condensation point b_c for this system is found to occur at $b_c = 1$. Thus the system never enters into the gel phase. Nevertheless, asymptotically as $b \to 1$ the experimental distributions are found to have the form (eq 10), viz., $(X_n/X) = q_0 n^{-\tau} F(\epsilon n^{\sigma})$, where $F(\epsilon n^{\sigma}) \to 1$ as $\epsilon \to 0$. This finding permits us to deduce the critical exponent τ,[16] and we have found $\tau = 1.4 \pm 0.15$.

It is difficult to deduce the exponent γ_g directly from the measured X_n's. To obtain γ_g one must accurately evaluate the sum $\sum_0^\infty n^2 X_n$ as b approaches unity. To reliably evaluate this sum, it is necessary that X_n be known accurately for values of n larger than those shown in the data of Figure 1. In fact, it is necessary to know X_n in a region of n for which $F(\epsilon n^{\sigma}) \ll 1$. To circumvent this difficulty we note that the X_n's closely follow the form of eq 5 as a function of b for $n = 1$–4. Also as $b \to 1$ this distribution agrees with data which extend to $n \sim 30$. If we assume then that eq 5 is an accurate representation of X_n/X for the entire range of values of n and b, we can compute the degree of polymerization $\mathrm{DP_w}$ which is essentially the second moment of the cluster size distribution. This is found to vary with b over the entire domain of b as $\mathrm{DP_w} = 1/(1-b)^2$ which signifies that the critical exponent[16] γ_g is equal to 2.

Also, as $b \to 1$ the distribution of eq 5 can be used to obtain the limiting form of $F(n,b)$ as $b \to 1$ from below. Since in this analysis b is restricted to values of $b < 1$, the validity of a power series expansion for F about $b = 1$ is clearly open to question. Keeping this reservation in mind the form of $F(nb)$ is found to be $F(n,b) \to (1 - n(1-b)^2/2 + \ldots)$ (as $b \to 1$), and this suggests provisionally that the critical exponent σ be assigned the value $^1/_2$.

The distribution which we have found experimentally is the same as that predicted for an equilibrium distribution of condensing monomers of the form $\mathcal{A}R\mathcal{B}_{f-1}$ in the limit $f \gg n$. Such monomers contain one $\mathcal{A}$ site and $f-1$ $\mathcal{B}$ sites and bonding may take place only between $\mathcal{A}$ and $\mathcal{B}$ sites. Also, our distribution is in agreement with the solution of the unidirectional generalized von Smoluchowski kinetic equations[15] provided that the bimolecular reaction rate constants have the form $a_{nn'} = B(n + n')$. Here n and n' are the number of monomers in each of the reacting clusters. Our results are markedly different from the distribution of identical polyfunctional units of the form $R\mathcal{A}_f$ in the limit $f \gg n$. For finite f, this system obeys the well-known Flory–Stockmayer distribution. Our values of σ and γ_g are close to those predicted by three-dimensional percholation theory (see Table I), but our value of τ is distinctly different from the predictions of that theory.

These experimental and theoretical findings make it clear that the exponents which describe the form and the moments of the cluster size distribution in the vicinity of the critical condensation point will depend markedly on

the allowed forms of interaction between the condensing monomers.

Finally, we compare the structure of our monomers with those appropriate to the theoretical models mentioned above. The binding of bifunctional antibody molecules to some of the f antigenic sites on each of the carrier particles produces monomers having on average $\bar{e}$ $\mathcal{A}$ type (active singly bonded antibody) sites and on average $f - \bar{e}$ $\mathcal{B}$ type (unlinked antigen) sites. The monomers interact by forming bonds between $\mathcal{A}$ and $\mathcal{B}$ sites. Each monomer thus is of the form $\mathcal{A}_e R \mathcal{B}_{f-e}$ where e is distributed among the monomers according to a Poisson distribution having as its mean $\bar{e}$. Using a method described previously,[26] we have determined that in the present experiments the smallest value of $\bar{e} = 10$ and the largest value is $\bar{e} = f/2$. It remains to be seen how such a distribution of high functionality monomers ($f \sim 10^3$) can interact kinetically or statistically so as to produce the experimentally observed cluster size distributions.

Acknowledgment. The authors thank Dr. Hans Hager of the Hoffmann-La Roche Company for kindly providing hSA coated latex spheres and goat anti-hSA antibody, Dr. Kurt Binder for helpful clarifying discussions on critical exponents in the percolation theory, and Dr. Richard Cohen for numerous helpful discussions of the theory of condensation of high functionality monomers. This work was supported by the Center for Materials Sciences and Engineering, M.I.T., under Contract DMR 78-24185, by the National Science Foundation under Grant PCM-7709031, and by the Whitaker Health Sciences Fund. Dr. von Schulthess acknowledges with thanks financial support from the Whitaker Health Sciences Fund, the Geigy Jubilaeums-Stiftung of Basel, the Steo-Stiftung of Zurich, and the Swiss National Science Foundation.

References and Notes

(1) P. J. Flory, *J. Am. Chem. Soc.*, **63**, 3083 (1941).
(2) P. J. Flory, "Principles of Polymer Chemistry", Cornell University Press, Ithaca, N.Y. 1953.
(3) W. Stockmayer, *J. Chem. Phys.*, **11**, 45 (1943).
(4) M. Gordon, *Proc. R. Soc. London, Ser. A*, **268**, 240 (1962).
(5) R. Goldberg, *J. Am. Chem. Soc.*, **74**, 5715 (1952).
(6) R. Aladjem and M. T. Parmiter, *J. Theor. Biol.*, **8**, 8 (1965).
(7) C. De Lisi, *J. Theor. Biol.*, **45**, 555 (1974).
(8) M. E. Fisher and J. W. Essam, *J. Math. Phys.*, **2**, 609 (1961).
(9) H. L. Frisch and J. M. Hammersley, *J. Soc. Ind. Appl. Math.*, **11**, 894 (1963).
(10) J. W. Essam in "Phase Transitions and Critical Phenomena", Vol. II, C. Domb and M. S. Green, Eds., Academic Press, New York, 1972, Chapter 6.
(11) M. E. Fisher, *Physics (N.Y.)*, **3**, 255 (1967).
(12) C. S. Kiang and D. Stauffer, *Z. Phys.*, **235**, 130 (1970).
(13) R. A. Cowley, G. Shirane, R. Birgeneau, and E. C. Svennson, *Phys. Rev. Lett.*, **39**, 894 (1977).
(14) *Discuss. Faraday Soc.*, **42**, 120 (1967).
(15) R. L. Drake in "Topics in Current Aerosol Research", Part 2, Vol. 3, G. M. Hidy and J. R. Brock, Eds., Pergamon Press, New York, 1972.
(16) D. Stauffer, *J. Chem. Soc., Faraday Trans. 2*, **72**, 1354 (1976).
(17) P. G. de Gennes, *J. Phys. Lett.*, **40**, L197 (1979).
(18) M. E. Levenstein, M. S. Shur, and A. L. Efros, *Zhr. Eksp. Teor. Fiz.*, **69**, 2023 (1975).
(19) M. von Smoluchowski, *Z. Phys. Chem.*, **42**, 129 (1918); see also S. Chandrasekhar, *Rev. Mod. Phys.*, **15**, 1 (1943).
(20) J. B. Mc Leod, *Q. J. Mech. Appl. Math.*, **13**, 119 (1962).
(21) A. H. Golovin, *Izv. Geophys. Ser. 5*, 482 (1963) (translated by F. Goodspeed).
(22) A. A. Lushnikov, *J. Colloid Interface Sci.*, **63** (2), 276 (1978).
(23) R. W. De Blois and C. P. Bean, *Rev. Sci. Instrum.*, **41**, 909 (1970).
(24) R. W. De Blois, C. P. Bean, and R. K. Wesley, *J. Colloid Interface Sci.*, **61** (2), 323 (1977).
(25) R. Cohen and G. B. Benedek, *Immunochemistry*, **12**, 349 (1975).
(26) G. von Schulthess, R. Cohen, N. Sakato, and G. Benedek, *Immunochemistry*, **13**, 955 (1976).
(27) G. von Schulthess, R. Cohen, and G. B. Benedek, *Immunochemistry*, **13**, 963 (1976).
(28) G. von Schulthess, M. Giglio, D. Cannell, and G. Benedek, *Mol. Immunol.*, in press.
(29) G. von Schulthess, *Biophys. J.*, **21**, 115A (1978).
(30) D. C. Golibersuch, *Biophys. J.*, **13**, 265 (1973).
(31) G. von Schulthess, Ph.D. Thesis, M.I.T. Department of Physics, Sept 1979.
(32) W. H. Stockmayer, *J. Chem. Phys.*, **12**, 125 (1944).
(33) R. J. Cohen and G. B. Benedek, in preparation.